Development 138, 2903-2908 (2011) doi:10.1242/dev.060269

Symmetry breaking in mouse oocytes requires transient F-actin meshwork destabilization

Jessica Azoury[1], Karen Wingman Lee[1], Virginie Georget[2], Pascale Hikal[1] and Marie-Hélène Verlhac[1,*,†]

SUMMARY

Female meiotic divisions are extremely asymmetric, giving rise to a large oocyte and small degenerating polar bodies, keeping the maternal stores for further embryo development. This asymmetry is achieved via off-center positioning of the division spindle. Mouse oocytes have developed a formin-2-dependent actin-based spindle positioning mechanism that allows the meiotic spindle to migrate towards the closest cortex. Using spinning disk microscopy and FRAP analysis, we studied the changes in the organization of the cytoplasmic F-actin meshwork during the first meiotic division. It is very dense in prophase I, undergoes a significant density drop upon meiosis resumption and reforms progressively later on. This meshwork remodeling correlates with endogenous formin 2 regulation. High formin 2 levels at meiosis I entry induce meshwork maintenance, leading to equal forces being exerted on the chromosomes, preventing spindle migration. Hence, the meshwork density drop at meiosis resumption is germane to the symmetry-breaking event required for successful asymmetric meiotic divisions.

KEY WORDS: F-actin, Asymmetric division, Meiosis, Mouse, Oocyte

INTRODUCTION

Asymmetric cell division requires correct spindle positioning with regards to the polarity axis of the mother cell (Gonczy, 2008). In most models, mitotic spindle positioning depends on pulling forces produced by astral microtubules that connect the centrosomes at spindle poles to the cell cortex. However, meiotic spindles in oocytes are often devoid of canonical centrosomes and astral microtubules (Szöllösi et al., 1972). Hence, alternative spindle positioning mechanisms are predominant. Prophase I mouse oocytes have a central nucleus and show no sign of polarization (FitzHarris et al., 2007; Halet and Carroll, 2007; Johnson, 2009). Instead, oocyte polarity is acquired after meiosis resumption as the first meiotic spindle moves along its long axis from the center towards the closest cortex (Verlhac et al., 2000a). This migration depends on the presence of a formin 2 (Fmn2)-nucleated cytoplasmic meshwork of F-actin filaments (Leader et al., 2002; Dumont et al., 2007a; Azoury et al., 2008; Schuh and Ellenberg, 2008). In its absence, spindle migration and asymmetric meiotic divisions are compromised (Brunet and Verlhac, 2011).

Despite its importance, the regulation of the F-actin meshwork is still poorly understood and it is currently unknown why first meiotic spindle migration takes place late in meiosis I. Organization and dynamics of F-actin as well as Fmn2 regulation were studied in maturing oocytes. The F-actin meshwork, which is dense in prophase I, undergoes an important density drop upon meiosis resumption, then reforms in late meiosis I. This meshwork remodeling correlates with Fmn2 degradation and reaccumulation. By maintaining high Fmn2 levels at meiosis resumption the meshwork density is maintained and spindle migration is compromised. Therefore, F-actin remodeling upon meiosis entry is essential for symmetry breaking in mouse oocytes.

[1]UMR7622, CNRS/UMPC, 9 quai Saint Bernard, 75005 Paris, France. [2]UMR5237, Montpellier RIO Imaging, 1919 route de Mende, 34000 Montpellier, France.

*Present address: CIRB, UMR-CNRS7241/INSERM U1050, Collège de France, 11 place Marcelin Berthelot, 75005 Paris, France
†Author for correspondence (marie-helene.verlhac@college-de-france.fr)

Accepted 4 May 2011

MATERIALS AND METHODS

Oocyte collection, culture and microinjection

Oocytes were collected from 11-week-old OF1 and *Fmn2*$^{-/-}$ female mice as described by Verlhac et al. (Verlhac et al., 1994). Oocytes were maintained at prophase I in M2+BSA medium containing 1 μM milrinone (Reis et al., 2006) and microinjected with cRNA using an Eppendorf Femtojet microinjector. NEBD was triggered by releasing oocytes into milrinone-free M2+BSA. Bortezomib (Selleck Chemicals) was stored in DMSO (10 mM) and diluted in M2+BSA at 0.1 μM.

Plasmid construction and in vitro transcription of synthetic RNA

We used the following constructs: pspe3-Utr-GFP and pRN3-actin-YFP (Azoury et al., 2008), pRN3-Rango-YFP (Dumont et al., 2007b), pRN3-histone-RFP (Tsurumi et al., 2004). pCS2-Myc-Fmn2 and pRN3-Fmn2-GFP [gifts from Philip Leder (Harvard Medical School, Boston, USA) and Rong Li (Stowers Institute for Medical Research, Kansas City, USA)]. The cRNA were synthesized as described previously (Verlhac et al., 2000b). To induce Fmn2-GFP or histone-RFP overexpression, cRNA were further poly(A) tailed using the Poly(A)-tailing kit (Ambion).

Immunoblotting and immunofluorescence

Immunoblotting of oocytes was performed as described previously (Terret et al., 2003). The anti-Fmn2 antibody (1:100) was directed and purified against two peptides NH_2-CGPRDAEITKKASGS-$COHN_2$ and NH_2-CRQKKGKSLYKVKPR-$CONH_2$ (Covalab). Oocytes were fixed in 4% paraformaldehyde in PBS for 30 minutes at 30°C.

Live confocal video microscopy

Spinning disk images were acquired using a Plan-APO 40×/1.25 NA objective on a Leica DMI6000B microscope enclosed in a thermostatic chamber (Life Imaging Service) equipped with a CoolSnap HQ2/CCD-camera coupled to a Sutter filter wheel (Roper Scientific) and a Yokogawa CSU-X1-M1. Metamorph (Universal Imaging) was used to collect data and ImageJ (NIH) to analyze and process data. Microfilament length was measured on three-dimensional images using the Volocity software.

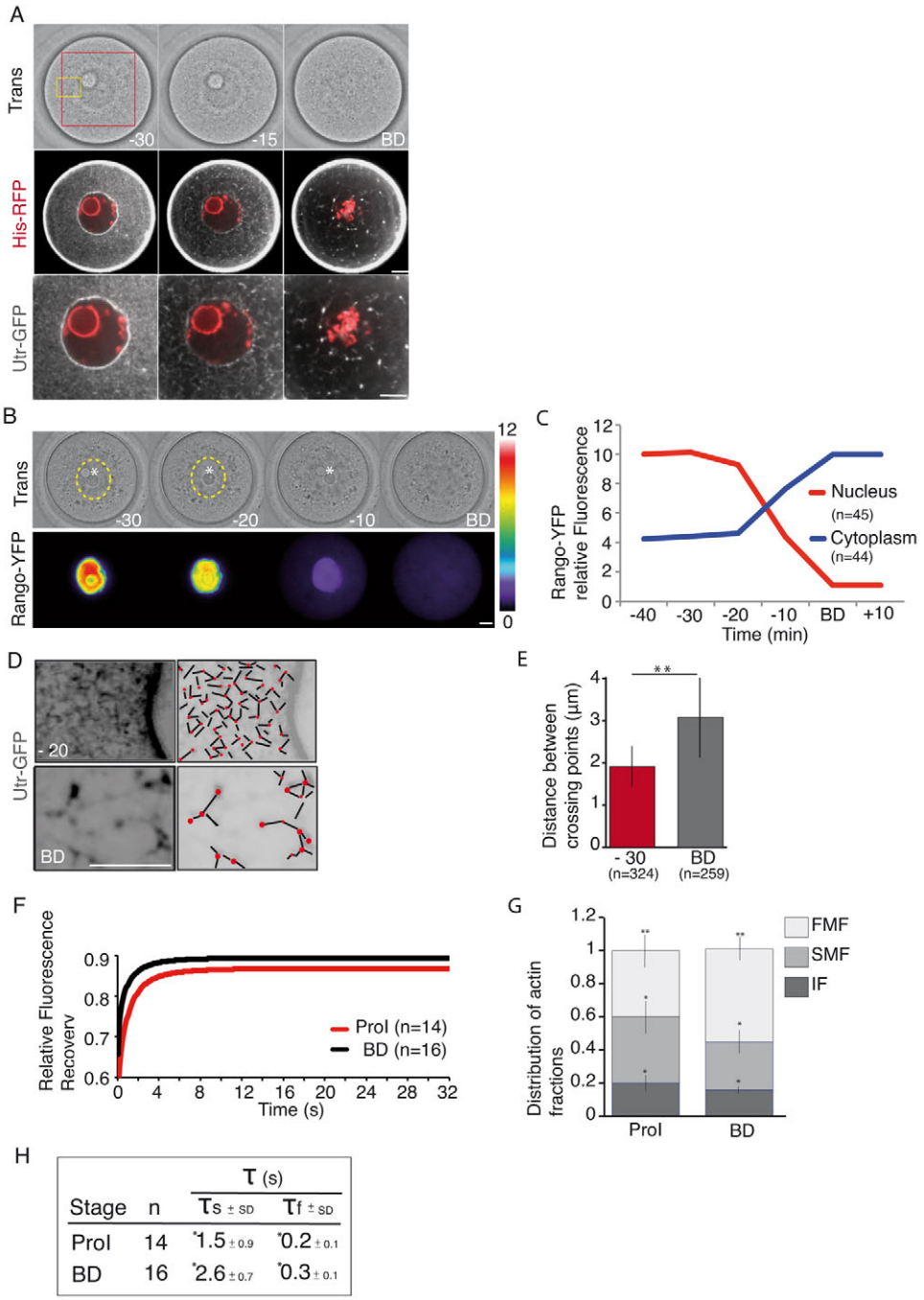

Fig. 1. The F-actin meshwork present in prophase I is remodeled at NEBD. (**A**) Time-lapse confocal microscopy of wild-type oocytes expressing Utr-GFP and histone-RFP at NEBD (*n*=76; more than three independent experiments). Trans, Transmitted light images. Bottom row: higher magnification of the region outlined by the red square. Times to breakdown (BD) is in minutes. Scale bars: 10 µm. (**B**) The nuclear probe, Rango, leaks out of the nucleus before NEBD. (Top row) Transmitted light images (*n*=45; three independent experiments). Dotted circles outline the nuclear envelope and the white asterisks indicates the nucleolus. Times to BD is in minutes. (Bottom row) Pseudocolored images: black, lowest intensity; white, highest intensity. Scale bar: 10 µm. (**C**) Graph representing the changes in fluorescence of Rango before (–) or after (+) NEBD, observed in bright-field images. Red curve, nuclear fluorescence; blue curve, cytoplasmic fluorescence. (**D**) Higher magnification of the region outlined by the yellow rectangle in A showing oocytes expressing Utr-GFP 20 minutes before and at NEBD. The right panels show actin microfilaments (black lines) and crossing points (red dots). Scale bar: 10 µm. (**E**) Bar graph representing the length of actin microfilaments between crossing points. *n*=number of filaments. Significant statistical difference was assessed with a *t*-test with a confidence interval of 95% (**P<0.001). (**F**) Mathematically fitted curves of FRAP of actin-YFP in the cytoplasm of oocytes over time. Prophase I (Pro I; red curve) and NEBD (black curve). (**G**) Bar graph showing the distribution of the different actin fractions in the cytoplasm at prophase I (*n*=14) and NEBD (*n*=16) oocytes. SMF, slow mobile fraction; FMF, fast mobile fraction; IF, immobile fraction =1–(SMF+FMF). Significant statistical difference was assessed as in E (*P<0.05; **P<0.001). (**H**) Table showing measures of τ_s and τ_f in the cytoplasm of prophase I and NEBD oocytes. τ_s is the time when 63% of the SMF has recovered. The lower the τ_s, the more dynamic the microfilaments. τ_f is to the time when 63% of the FMF has recovered. *P<0.05.

Quantification of endogenous Fmn2 cortical staining was performed on maximal projections of ten *z*-planes, separated by 1 μm. After background subtraction, cortical intensity was measured and averaged (six line scans/oocyte).

Nuclear shape analysis was performed on Ran-regulated importin-β cargo (Rango)-expressing oocytes (maximal projections of five *z*-planes each 3 μm). Nuclear fluorescence was thresholded and automatically tracked in the *x*-*y* plane (Metamorph). The circularity shape factor represents the degree of deviation of a certain shape from an ideal circle (0-1; ideal circle=1). It is a function of the perimeter P and the area A: $f_{circ}=4\pi A/P^2$.

Because nuclear shape is influenced by Fmn2 levels, nuclear position (ρ) was measured slightly differently, as described by Brunet and Maro (Brunet and Maro, 2007). It was calculated in Rango-expressing oocytes as the ratio (distance between oocyte and nucleus centroids) / (difference between oocyte and nuclear surfaces) × 10,000.

Fluorescence recovery after photobleaching experiments

Fluorescence recovery after photobleaching (FRAP) was performed as described previously (Azoury et al., 2008). The recovery of actin-YFP after photobleaching depends on the dynamics of the microfilaments in which it is incorporated. We assume that the slow mobile fraction (SMF) corresponds to actin-YFP integrated into polymerizing microfilaments and that the fast mobile fraction (FMF) corresponds to freely diffusing G-actin-YFP. The immobile fraction (IF) can be interpreted as a fraction of stable F-actin turning over slowly.

RESULTS AND DISCUSSION

We and others have shown that a dynamic cytoplasmic actin microfilament meshwork is required for spindle migration. To assess its organizational changes, oocytes expressing the F-actin-specific probe, Utr-CH-GFP (Burkel et al., 2007), were imaged. A dense F-actin meshwork connecting the nucleus to the cortex was present in prophase-I-arrested oocytes (Fig. 1A). The meshwork density dropped globally before signs of nuclear envelope breakdown (NEBD) were visible in bright-field images (Fig. 1A; see Movie 1 in the supplementary material). To examine a potential correlation between these two events, oocytes expressing Rango, a probe known to accumulate in the nucleus, were imaged during prophase I exit (Kalab et al., 2006; Dumont et al., 2007b). Rango leaked into the cytoplasm before NEBD was seen under bright-field illumination (Fig. 1B,C; see Movie 2 in the supplementary

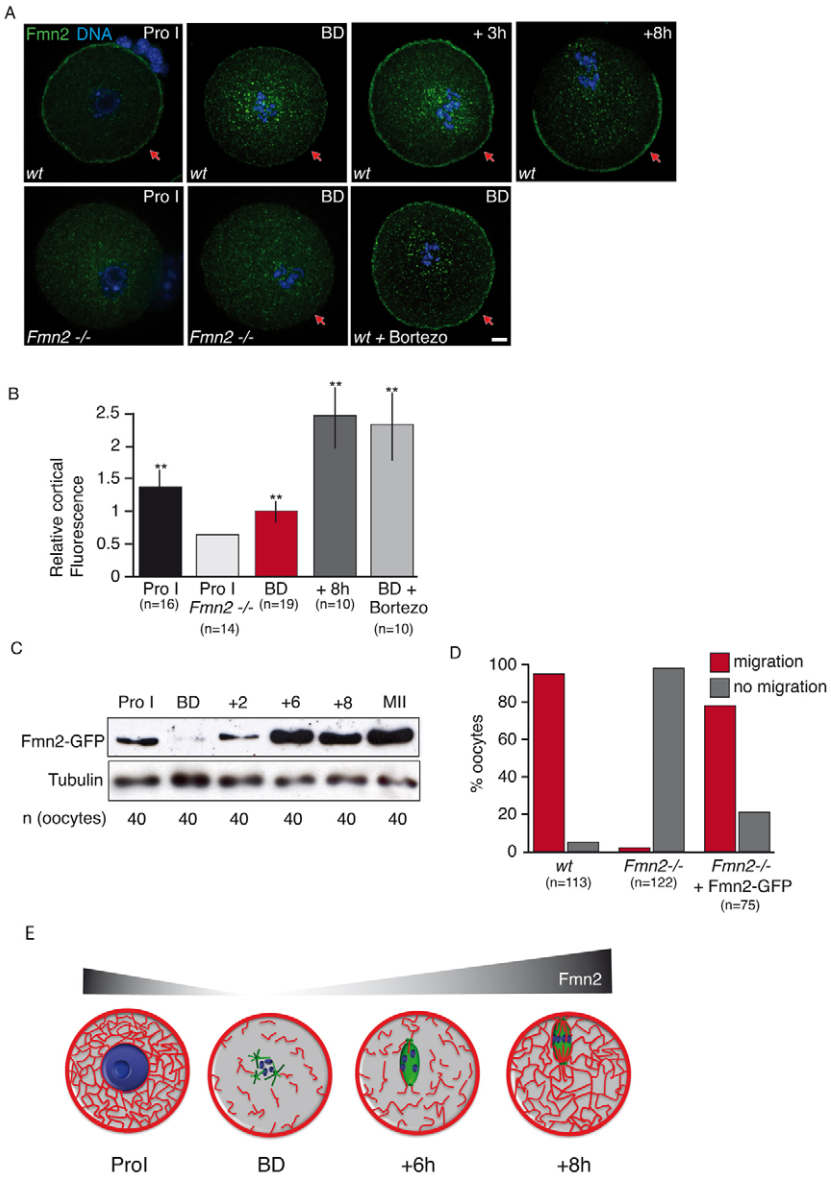

Fig. 2. Correlation between Fmn2 regulation and meshwork remodeling during meiotic maturation. (**A**) Control wild-type and *Fmn2*$^{-/-}$ oocytes observed at different stages of meiotic maturation [prophase I (Pro I), NEBD, 3 hours and 8 hours after NEBD] using anti-Fmn2. *wt* + Bortezo, wild-type oocytes treated with 0.1 μM Bortezomib for 90 minutes before fixation. All oocytes were observed using the same settings and the images treated the same way (three independent experiments). Red arrows indicate cortical labeling. Scale bar: 10 μm. (**B**) Bar graph showing the average relative fluorescence of cortical Fmn2 from oocytes in A. The cortical fluorescence of each oocyte was divided by the average cortical fluorescence at NEBD (**P<0.0005). (**C**) Extracts from oocytes expressing Fmn2-GFP were obtained at different time points of meiotic maturation (Pro I; NEBD; 2, 6 and 8 hours after BD and at metaphase II; MII) and immunoblotted using anti-GFP and anti-tubulin (loading control). The results are from three independent experiments. (**D**) Bar graph showing the percentage of chromosome migration in wild-type, *Fmn2*$^{-/-}$ and *Fmn2*$^{-/-}$ oocytes injected with Fmn2-GFP. The results are from three independent experiments. (**E**) A schematic showing the correlation between the presence of Fmn2 and the cytoplasmic F-actin meshwork remodeling during meiotic maturation. Chromosomes are shown in blue, microtubules in green and actin in red.

material), as in starfish oocytes (Lenart et al., 2003). Therefore, the decrease in meshwork density is concomitant with the increase in nuclear envelope permeability. This drop was associated with an increase in filament length from 2 to 3 μm (Fig. 1D,E) and a reduction of filamentous actin (SMF+IF) relative to G-actin (FMF; Fig. 1F,G) as shown by FRAP on actin-YFP. The remaining F-actin was less dynamic at NEBD, with higher τ_s values (the time when 63% of the SMF has recovered; Fig. 1H). Using two approaches, we show that F-actin meshwork density and dynamics decrease upon meiosis resumption.

Late meiosis I cytoplasmic meshwork reformation requires Fmn2. Endogenous Fmn2, localized in the cortex of prophase I oocytes, disappeared at NEBD, reappeared later and was enriched in the cortex opposite the spindle (Fig. 2A,B). *Fmn2*$^{-/-}$ oocytes lacked cortical Fmn2 staining, suggesting that the staining is specific (Fig. 2A,B). Cortical localization was maintained at NEBD in wild-type oocytes treated with the proteasome inhibitor, Bortezomib (Lightcap et al., 2000), indicating that Fmn2 is degraded at NEBD (Fig. 2A,B). We also observed a reduction in cortical exogenous Fmn2-GFP labeling at NEBD (data not shown) (Schuh and Ellenberg, 2008). Immunoblotting of exogenous Fmn2-GFP confirmed that Fmn2 was degraded at NEBD (twofold to fivefold drop; Fig. 3A,B) and reaccumulated later (Fig. 2C). Furthermore, Fmn2-GFP mimics endogenous Fmn2, because injected Fmn2-GFP efficiently rescued spindle migration in *Fmn2*$^{-/-}$ oocytes (Fig. 2D), and in rescued oocytes, the intensity of exogenous Fmn2-GFP cortical signal (6.4±1.4, arbitrary units; detected with the anti-Fmn2 antibody) was comparable with the endogenous levels in wild-type oocytes (7.6±1.8). Therefore, the correlation between the meshwork and Fmn2 changes (Fig. 2E) potentially explains why spindle migration occurs late in meiosis I.

What is the biological relevance of dismantling the meshwork and rebuilding it later? To address this, we wished to promote meshwork maintenance at meiosis entry by overexpressing Fmn2. Fmn2-GFP overexpression (Fmn2 O/E) prevented the reduction in Fmn2 levels normally observed at NEBD (Fig. 3A,B). Fmn2 O/E oocytes had a stronger Fmn2 cortical labeling (1.5× higher than that of Fmn2-GFP; Fig. 3C). In addition, actin filaments surrounding the nucleus, as well as cytoplasmic ones, were maintained at NEBD (Fig. 3D; see Movie 3 in the supplementary material). The filament length remained unchanged (Fig. 3E), and FRAP analysis showed similar microfilament dynamics in prophase I and at NEBD (Fig. 3F). Our data prove that Fmn2 overexpression maintained the F-actin meshwork at meiosis resumption. Did it alter subsequent organization? Although more

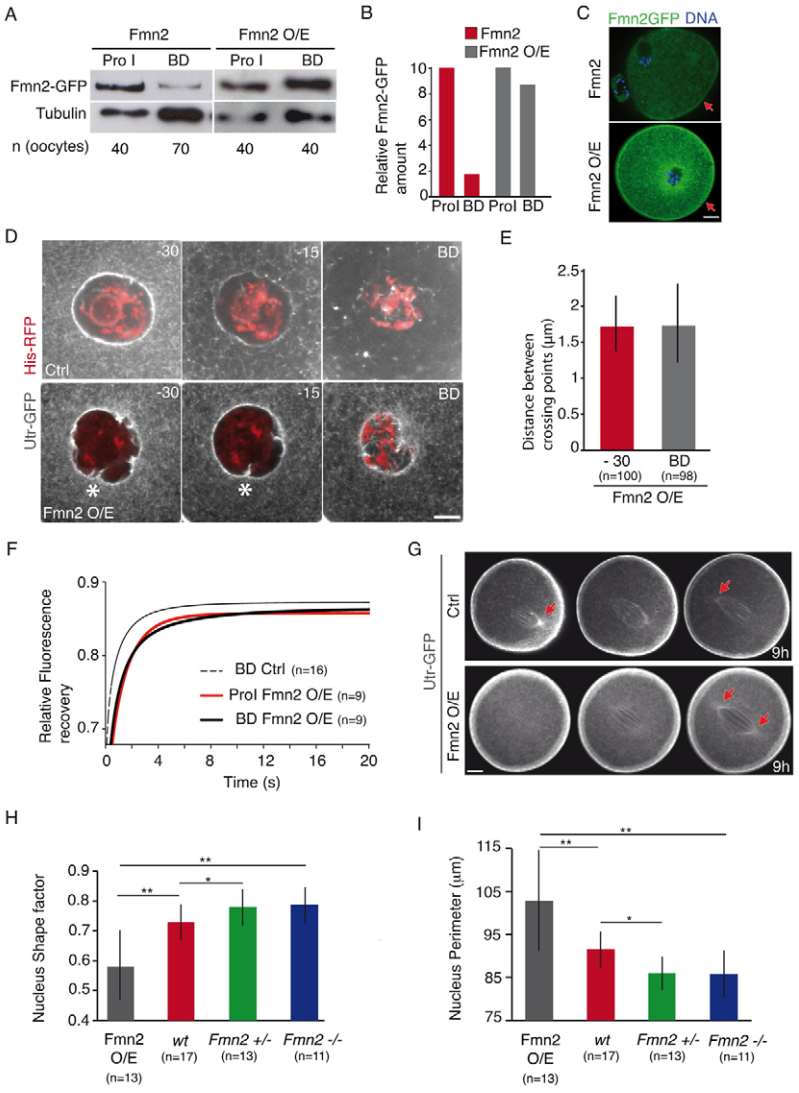

Fig. 3. Overexpressing Fmn2 maintains the F-actin meshwork and induces nuclear deformations. (**A**) Extracts of oocytes expressing Fmn2-GFP (left) or overexpressing Fmn2-GFP (Fmn2 O/E; right) at prophase I and NEBD were immunoblotted using anti-GFP and anti-tubulin (loading control). The results are from three independent experiments. (**B**) Bar graph showing the relative drop in Fmn2-GFP at NEBD compared with prophase I in oocytes expressing Fmn2-GFP or Fmn2-GFP O/E. (**C**) Oocytes expressing Fmn2-GFP or Fmn2-GFP O/E at 14 hours after NEBD (same settings). Fmn2 labeling is shown in green and DNA in blue; red arrows indicate Fmn2 cortical labeling. Scale bar: 10 μm. (**D**) Time-lapse confocal microscopy of Utr-GFP and histone-RFP expression at NEBD in control (*n*=76) and Myc-Fmn2 overexpressing (Fmn2 O/E) oocytes (*n*=21; three independent experiments). The white asterisks indicate nuclear invaginations. Times to BD is in minutes. Scale bar: 10 μm. (**E**) Bar graph representing the length of actin microfilaments between crossing points. *n*=filaments number. Error bars indicate s.d. (**F**) Mathematically fitted curves of FRAP of actin-YFP in the cytoplasm of oocytes over time. Prophase I (red curve) and NEBD (black curve) of oocytes overexpressing Myc-Fmn2. (**G**) Representative images of Utr-GFP-expressing (control) and Myc-Fmn2O/E oocytes at late meiosis I (MI). Three *z*-planes, spaced of 4 μm, are shown. Red arrows indicate spindle poles. Scale bar: 10 μm. (**H**,**I**) Bar graphs representing (H) the circularity shape factor and (I) the perimeter of nuclei in *Fmn2*$^{-/-}$, *Fmn2*$^{+/-}$, wild-type and Myc-Fmn2 O/E oocytes. $^{**}P<0.005$; $^{*}P<0.05$.

microfilaments connected the spindle pole facing the closest cortex in controls, the meshwork was no longer asymmetrically distributed: microfilaments connected both spindle poles equally to the cortex in Fmn2 O/E oocytes (Fig. 3G).

In Fmn2 O/E oocytes, nuclei appeared to have deformations, as if they were subjected to external forces (Fig. 3D, asterisks; see Movie 3 in the supplementary material). Therefore, the radius, circularity and perimeter were quantified. The mean radius was similar in *Fmn2*$^{-/-}$, *Fmn2*$^{+/-}$, wild-type and Fmn2 O/E oocytes (11.87±0.42, 11.97±0.33, 12.20±0.44 and 12.14±0.30 μm, respectively) suggesting that nuclei had comparable volumes. Although the nucleus circularity shape factor was closest to 1 (1 corresponding to a circle) in *Fmn2*$^{-/-}$ oocytes (Fig. 3H), the longest perimeter was observed in Fmn2 O/E oocytes (Fig. 3I), proving that nuclear deformations increased with the amount of Fmn2 (Fig. 3H,I). Therefore, the amount of Fmn2 controls the density of the meshwork and the extent of the external forces applied on the nucleus: the more Fmn2, the denser the meshwork, the greater the forces.

Stabilizing the meshwork around the nucleus and applying more forces to it has no effect on the percentage, timing of NEBD or kinetics of nuclear permeability (see Fig. S1 in the supplementary material) but impaired nucleus and spindle positioning. We observed a correlation between the amount of Fmn2 and the position of the nucleus: nuclei were more off-center in *Fmn2*$^{-/-}$ oocytes, consistent with earlier work (Dumont et al., 2007a), than in Fmn2 O/E oocytes (Fig. 4A). Also, in 65% of Fmn2 O/E oocytes, chromosome migration did not occur (Fig. 4B,C) and subsequent asymmetry of division was compromised (see Fig. S2A in the supplementary material). Therefore, symmetrical spindle pole anchorage to the cortex in late meiosis I greatly influenced spindle positioning without affecting meiotic spindle assembly per se (Fig. 4D; see Fig. S2B-D in the supplementary material).

In prophase I, F-actin physically connects the nucleus to the cortex and exerts balanced forces leading to its centering. Dramatic destabilization of F-actin at metaphase entry has never before been documented in mitotic cells, which use both microtubule- and actin-based spindle positioning systems (Woolner et al., 2008). The meshwork remodeling correlates with Fmn2 regulation. Little is known about regulation of non-mDiaphanous-related formins (Goode and Eck, 2007) and there is only one example of formin regulation via degradation (DeWard and Alberts, 2009). Yet, degradation might be a more general means of controlling formin activity in vivo.

Two strictly opposing phenomena, the absence (in *Fmn2*$^{-/-}$ cells) or continuous presence (Fmn2 O/E cells) of cytoplasmic F-actin meshwork, end up producing the same chromosome-positioning defect (see Fig. S2E in the supplementary material). We propose that in its absence, the forces are not transduced, therefore no chromosome movement occurs, whereas in its continuous presence, forces are balanced and symmetry breaking is prevented. Our work illustrates a novel means in generating unequal forces driving spindle migration and subsequent asymmetric division: destroying an existing symmetrical organization via degradation of one key element, followed by the re-forming of an asymmetrical one.

We show that Fmn2-nucleated microfilaments exert pushing forces because: (1) reducing Fmn2 levels increases nuclear off-centering, (2) increasing Fmn2 levels induces nuclear deformations compatible with pushing (invaginations) rather than pulling (extensions) forces and (3) endogenous Fmn2 accumulates in the cortex opposite the migrating spindle. Microfilaments that anchor the closest pole to the cortex (Azoury et al., 2008) and exert pulling forces (Schuh and Ellenberg, 2008) may depend on another nucleator, activated by the proximity of chromosomes and the presence of a RanGTP

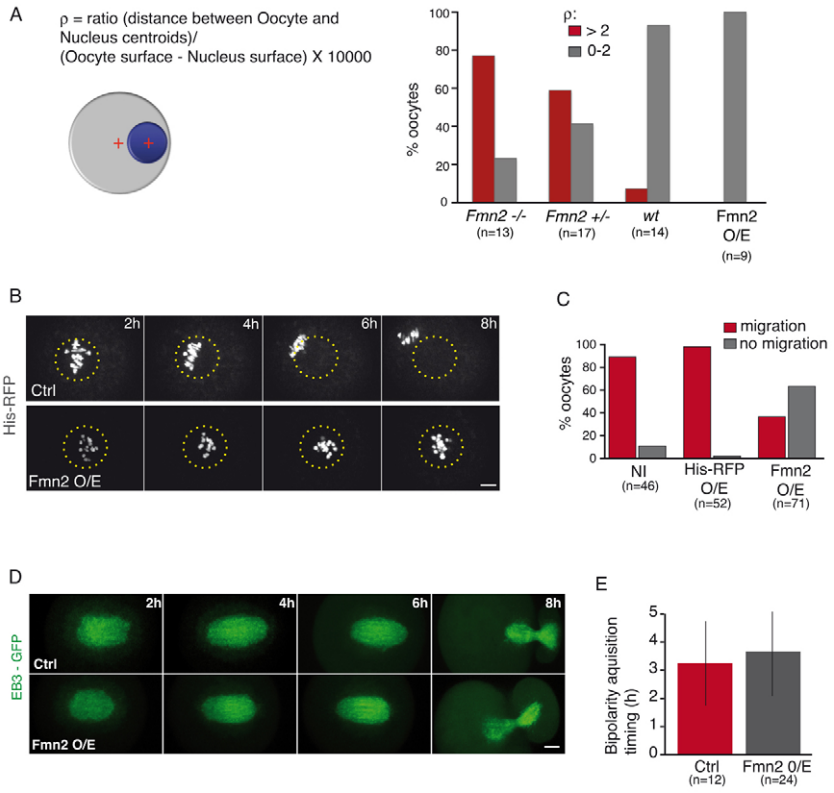

Fig. 4. Influence of the cytoplasmic meshwork on nucleus and spindle positioning. (**A**) Nucleus position as a function of the amount of Fmn2. (Left) Scheme representing oocyte and nucleus centroids. (Right) Bar graph showing the percentage of oocytes with ρ values below 2 or above 2 in different contexts. The higher the nuclear position (ρ), the more off-center the nucleus. (**B**) Time-lapse confocal images of histone-RFP-expression during meiotic maturation in control (*n*=41) and Fmn2-GFP O/E oocytes (*n*=45; three independent experiments). Dotted circles indicate initial position of chromosomes. Times after NEBD in hours. Scale bar: 10 μm. (**C**) Bar graph showing the percentage of chromosome migration in non-injected, histone-RFP-overexpressing (O/E) and Fmn2-GFP O/E oocytes. (**D**) Time-lapse confocal microscopy of EB3-GFP expression during meiotic maturation in control (*n*=46) and Myc-Fmn2 O/E oocytes (*n*=26; three independent experiments). Times after NEBD in hours. Scale bar: 10 μm. (**E**) Bar graph showing the timing of spindle bipolarity in control and Myc-Fmn2 O/E oocytes.

gradient (Deng et al., 2007; Dumont et al., 2007b). Our work reconciles a pushing (Li et al., 2008) and a pulling model (Schuh and Ellenberg, 2008) both of which are required for proper meiosis I spindle positioning to the cortex.

Acknowledgements
We thank Stéphane Brunet, Agnieszka Kolano and Marie-Emilie Terret for critical reading of the manuscript. This work was supported by grants from Ligue Nationale Contre le Cancer (Ligue Label EL/2009/LNCC) and Agence Nationale pour la Recherche (ANR08-BLAN-0136-01) to M.H.V. J.A. is the recipient of a fellowship from the Ministère délégué à la Recherche et aux Nouvelles Technologies.

Competing interests statement
The authors declare no competing financial interests.

Supplementary material
Supplementary material for this article is available at
http://dev.biologists.org/lookup/suppl/doi:10.1242/dev.060269/-/DC1

References
Azoury, J., Lee, K. W., Georget, V., Rassinier, P., Leader, B. and Verlhac, M.-H. (2008). Spindle positioning in mouse oocytes relies on a dynamic meshwork of actin filaments. *Curr. Biol.* **18**, 1514-1519.
Brunet, S. and Maro, B. (2007). Germinal vesicle position and meiotic maturation in mouse oocyte. *Reproduction* **133**, 1069-1072.
Brunet, S. and Verlhac, M.-H. (2011). Positioning to get out of meiosis: the asymmetry of division. *Hum. Reprod. Update* **17**, 68-75.
Burkel, B. M., von Dassow, G. and Bement, W. M. (2007). Versatile fluorescent probes for actin filaments based on the actin-binding domain of utrophin. *Cell Motil. Cytoskeleton* **64**, 822-832.
Deng, M., Suraneni, P., Schultz, R. M. and Li, R. (2007). The RanGTPase mediates chromatin signaling to control cortical polarity during polar body extrusion in mouse oocytes. *Dev. Cell* **12**, 301-308.
DeWard, A. D. and Alberts, A. S. (2009). Ubiquitin-mediated degradation of the formin mDia2 upon completion of cell division. *J. Biol. Chem.* **284**, 20061-20069.
Dumont, J., Million, K., Sunderland, K., Rassinier, P., Lim, H., Leader, B. and Verlhac, M.-H. (2007a). Formin-2 is required for spindle migration and for late steps of cytokinesis in mouse oocytes. *Dev. Biol.* **301**, 254-265.
Dumont, J., Petri, S., Pellegrin, F., Terret, M.-E., Bohnsack, M. T., Rassinier, P., Georget, V., Kalab, P., Gruss, O. J. and Verlhac, M.-H. (2007b). A centriole- and RanGTP-independent spindle assembly pathway in meiosis I of vertebrate oocytes. *J. Cell Biol.* **176**, 295-305.
FitzHarris, G., Marangos, P. and Carroll, J. (2007). Changes in endoplasmic reticulum structure during mouse oocyte maturation are controlled by the cytoskeleton and cytoplasmic dynein. *Dev. Biol.* **305**, 133-144.
Gonczy, P. (2008). Mechanisms of asymmetric cell division: flies and worms pave the way. *Nat. Rev. Mol. Cell Biol.* **9**, 355-366.
Goode, B. L. and Eck, M. J. (2007). Mechanism and function of formins in the control of actin assembly. *Annu. Rev. Biochem.* **76**, 593-627.
Halet, G. and Carroll, J. (2007). Rac activity is polarized and regulates meiotic spindle stability and anchoring in mammalian oocytes. *Dev. Cell* **12**, 309-317.
Johnson, M. H. (2009). From mouse egg to mouse embryo: polarities, axes, and tissues. *Annu. Rev. Cell Dev. Biol.* **25**, 483-512.
Kalab, P., Pralle, A., Isacoff, E. Y., Heald, R. and Weis, K. (2006). Analysis of a RanGTP-regulated gradient in mitotic somatic cells. *Nature* **440**, 697-701.
Leader, B., Lim, H., Carabatsos, M. J., Harrington, A., Ecsedy, J., Pellman, D., Maas, R. and Leder, P. (2002). Formin-2, polyploidy, hypofertility and positioning of the meiotic spindle in mouse oocytes. *Nat. Cell Biol.* **4**, 921-928.
Lenart, P., Rabut, G., Daigle, N., Hand, A. R., Terasaki, M. and Ellenberg, J. (2003). Nuclear envelope breakdown in starfish oocytes proceeds by partial NPC disassembly followed by a rapidly spreading fenestration of nuclear membranes. *J. Cell Biol.* **160**, 1055-1068.
Li, H., Guo, F., Rubinstein, B. and Li, R. (2008). Actin-driven chromosomal motility leads to symmetry breaking in mammalian meiotic oocytes. *Nat. Cell Biol.* **10**, 1301-1308.
Lightcap, E. S., McCormack, T. A., Pien, C. S., Chau, V., Adams, J. and Ellioth, P. J. (2000). Proteasome inhibition measurements: clinical application. *Clin. Chem.* **46**, 673-683.
Reis, A., Chang, H. Y., Levasseur, M. and Jones, K. T. (2006). APCcdh1 activity in mouse oocytes prevents entry into the first meiotic division. *Nat. Cell Biol.* **8**, 539-540.
Schuh, M. and Ellenberg, J. (2008). A new model for asymmetric spindle positioning in mouse oocytes. *Curr. Biol.* **18**, 1986-1992.
Szöllösi, D., Calarco, P. and Donahue, R. P. (1972). Absence of centrioles in the first and second meiotic spindles of mouse oocytes. *J. Cell Sci.* **11**, 521-541.
Terret, M.-E., Lefebvre, C., Djiane, A., Rassinier, P., Moreau, J., Maro, B. and Verlhac, M.-H. (2003). DOC1R: a MAP kinase substrate that control microtubule organization of metaphase II mouse oocytes. *Development* **130**, 5169-5177.
Tsurumi, C., Hoffmann, S., Geley, S., Graeser, R. and Polanski, Z. (2004). The spindle assembly checkpoint is not essential for CSF arrest of mouse oocytes. *J. Cell Biol.* **167**, 1037-1050.
Verlhac, M.-H., Kubiak, J. Z., Clarke, H. J. and Maro, B. (1994). Microtubule and chromatin behavior follow MAP kinase activity but not MPF activity during meiosis in mouse oocytes. *Development* **120**, 1017-1025.
Verlhac, M.-H., Lefebvre, C., Guillaud, P., Rassinier, P. and Maro, B. (2000a). Asymmetric division in mouse oocytes: with or without Mos. *Curr. Biol.* **10**, 1303-1306.
Verlhac, M. H., Lefebvre, C., Kubiak, J. Z., Umbhauer, M., Rassinier, P., Colledge, W. and Maro, B. (2000b). Mos activates MAP kinase in mouse oocytes through two opposite pathways. *EMBO J.* **19**, 6065-6074.
Woolner, S., O'Brien, L. L., Wiese, C. and Bement, W. M. (2008). Myosin-10 and actin filaments are essential for mitotic spindle function. *J. Cell Biol.* **182**, 77-88.